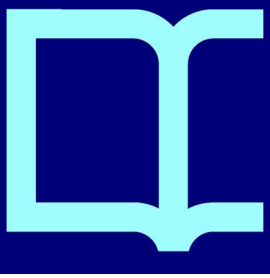

Inventory Robots: Performance Evaluation of an RFID-Based Navigation Strategy

S. López-Soriano and Rafael Pous, *Member, IEEE*

***Abstract*— Inventory robots produce accurate results while reducing costs. Such robots are specialized in navigating around store/warehouse facilities while reading radiofrequency identification (RFID) tags. However, commercial stores pose a serious challenge to navigation capabilities since these scenarios are likely to be modified relatively frequently. Current solutions involve having to re-map the modified layout and redesign the robots' routes. This means that a human operator must direct the robot through the target area, reducing the autonomy and scalability of these solutions. The main goals of this article are: first, assessing the feasibility of RFID-based exploration to enable autonomous mapping of inventory environments; and second, comparing the classical robotic navigation based on waypoints to the RFID-based navigation strategy. It will be shown that RFID-based strategies can be used to successfully build maps autonomously and obtain similar inventory accuracies when compared the current non-autonomous strategies.**

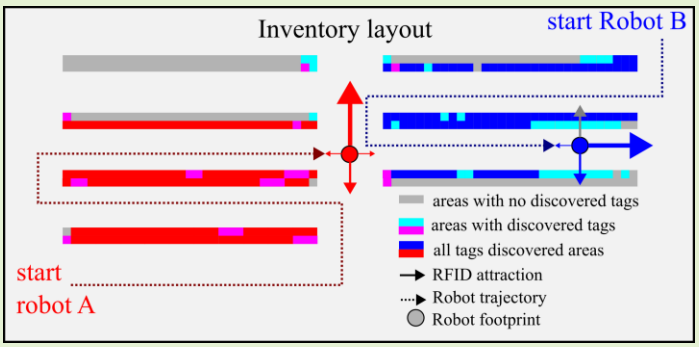

***Index Terms*— Inventory robots, RFID, exploration, navigation, e-logistics.**

I. Introduction

NOWADAYS, companies adopting robotic inventory solutions benefit from reducing inventory time and cost, and increasing their accuracy, eliminating human errors, having zero training time and consistent performance, and showing an innovative brand image [1], [2]. However, although there are many current solutions in the market, these robots are bulky (bothering customers) and expensive, which slows down the broad market adoption.

Besides, such solutions require an installation phase, which has a detrimental impact on the scalability. The reason is that robots require a map to localize themselves in the environment and a predefined route to navigate such space [3]. But current solutions for inventory robots require a human operator to build the map, i.e. to drive a robot throughout the target area [1], [4] while the robot is doing simultaneous localization and mapping (SLAM) [5]–[7]. This way the navigable area is bounded, and the mission route is optimized for a particular inventory layout. In later missions, the robot localizes itself on the map using the robot odometry and sensor measurements [5], [7].

S. López-Soriano was with the Department of Communications and Information Technology, Universitat Pompeu Fabra, Roc Boronat, 138, 08018 Barcelona, Spain. He is now with the Wireless Networks Group, Universitat Oberta de Catalunya, Rambla del Poblenou, 156, 08018 Barcelona, Spain (e-mail: slopezsor@uoc.edu).

Rafael Pous is with the Department of Communications and Information Technology, Universitat Pompeu Fabra, Roc Boronat, 138, 08018 Barcelona, Spain (e-mail: Rafael.pous@upf.edu).

To date, there are no commercial solutions or scientific papers that propose an autonomous exploration framework for inventory robots. The key to achieve fully autonomous inventory robots lies in their ability to autonomously map inventory environments. Hence, autonomous exploration is expected to solve the scalability issues of current solutions [8]. In the last years, there has been a huge interest for autonomous exploration and several techniques have been developed [3], [9]–[11]. These can be classified in frontier-based techniques [12], [13], metaheuristic algorithms [14], bio-inspired techniques [3], such as Particle Swarm Optimization (PSO), methods based on convolutional neural networks (CNNs) and deep reinforcement learning [15], and clustering techniques [16]. The main drawback of these techniques is that they still require a configuration phase to set the boundaries for the exploration area, otherwise the robots will extend the exploration area to the whole available area. Constrained exploration is essential for creating a map that is limited to the inventory area, which is crucial for enabling autonomous itinerary planning in RFID inventory environments. This type of mapping allows a robot to autonomously design its own inventory itinerary, composed of a set of waypoints starting from the initial position and crossing the layout-specific set of waypoints within the inventory environment's target area, up to the final location.

An exploration method based on the attraction of the robot towards the inventory items (RFID exploration) would

automatize the system installation processes and/or posterior system reconfigurations, this is required due to layout modifications. Moreover, such method is expected to enable autonomous optimization of itinerary planning for robotic inventory missions. Scilicet, autonomously designing a specific route, consisting in a series of autonomously generated waypoints, that maximizes the inventory accuracy. To that end, the RFID technology [17], used broadly in inventory applications [18]–[20], will be used as the backbone of the proposed exploration strategy for inventory applications.

RFID is one of the most used technologies for inventory processes globally, and it has been applied to robotics applications in the past [21]–[28]. RFID transponders are used to identify and locate items, machinery, humans, etc. During the last two decades, RFID technology has been used in robotics for localizing robots and items [21], [22], trajectory-tracking [23], navigation [24], [25], obstacle avoidance [26], autonomous exploration of unmapped areas [27], [28], etc. In [24], the authors propose a coverage algorithm that optimizes the exploration task by balancing multiple criteria in low tag density scenarios. However, the scalability problem is not solved since it assumes the possession of a known map. In addition, inventory is a high tag density problem, which is not assessed in this study. In [27], robots autonomously deploy RFID tags along their trajectories to coordinate the multi-robot exploration respectively. The approach suggested in [28] proposes an RFID-based navigation strategy, also called RFID stigmergy, to tackle the inventory problem for autonomous collaborative robots. RFID-based navigation requires low computation, and it does not require a configuration phase. However, RFID-based navigation hasn't been compared to the classical navigation approach using a predefined route.

The goals of this work are: first, developing an autonomous exploration method based on the RFID technology that enables to produce maps of inventory layouts with constrained boundaries, and second, comparing the classical waypoint navigation [29] to the RFID-based navigation and analyze the results. Thus, this document provides the following contributions:

1) the first demonstration of the efficacy of RFID-based autonomous exploration for optimizing the mapping of the target area in inventory environments,
2) an experimental comparison between the waypoint navigation and the RFID-based navigation.

In the following sections, it will be demonstrated that RFID-based exploration can be used to build maps of unknown real-life scenarios autonomously, and such resulting maps are well fitted for inventory missions (i.e., the map limits approach the boundaries of the area required to navigate the inventory layout according to the classical map-based navigation using waypoints). To that end, the experiments included in this work are performed in a dynamic real scenario consisting of a library full of students, what is to say, including unpredictable dynamic obstacles during the experiments.

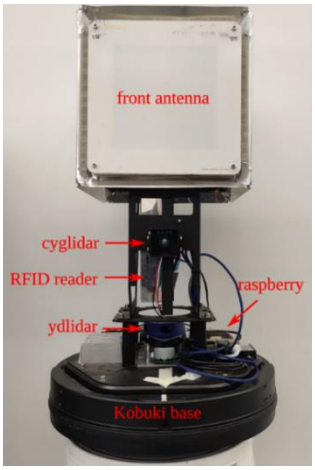

(a)

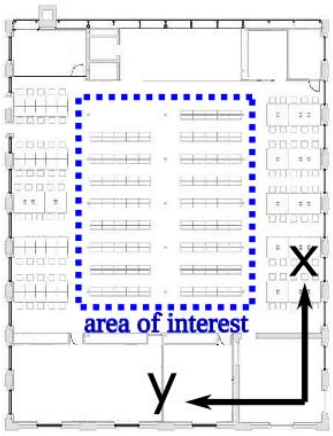

(b)

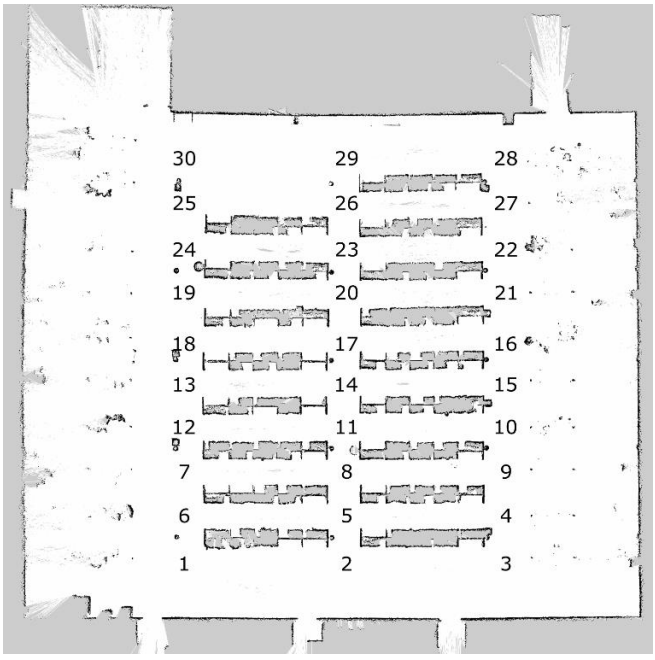

(c)

Fig.1. (a) Image of the robot prototype. (b) Layout of the library floor. The area of interest (blue dotted line) contains the shelves filled with the tagged items (books). (c) Map, containing the waypoints used for navigation, obtained by a human-driven robot prototype.

II. Materials and Application

Unlike current commercial solutions, the robot used for the experiments consists of a simple, small, and low-cost design. The prototype is shown in Fig.1(a). It consists of a commercial base [30], a raspberry pi4 model B [31], a cyglidar [32], a ydlidar [33], an RFID reader [34] and 4 reader antennas [35], oriented towards the front, left, back and right sides respectively.

The tests are conducted in the library of the Pompeu Fabra University [36]. The library is a dynamic scenario, where the items are books placed on shelves distributed throughout the room. Fig.1(b) illustrates the layout of the library floor. The whole room area is 21 x 19 m^2. The area of interest is 16 x 12 m^2 and contains two rows of 8 and 9 shelves filled with RFID tagged books. In total, there are 10 horizontal aisles and 3 vertical aisles. Fig.1(c) shows the map of the area, obtained by driving the robot across the environment. The ground truth (N_{gt}) has been carried out manually by a human operator and it consists of 6000 UHF RFID tags that univocally identify the tagged books.

The inventory performance [37] is assessed in terms of two parameters, namely the inventory accuracy (i_{acc}) and the inventory time (t_i). The inventory accuracy is calculated as (1), where N_{ic} is the inventory count (number of unique tags read during the inventory mission) and N_{gt} is the total number of tags in the ground truth. The inventory time is set to 100 minutes for the inventory performance to be compared in terms of i_{acc} amongst all proposed strategies.

$$i_{acc} = \frac{N_{ic}}{N_{gt}} \tag{1}$$

III. RFID-BASED EXPLORATION

In this section, we present a novel method for autonomous RFID-based exploration of inventory environments. The proposed methodology uses the ability of the robots to sense the RFID tags in different directions of the environment in a heuristic function (see equation 2), and it combines it with the concept of frontier-based exploration. This strategy is intended to explore, solely, the areas of interest of the inventory layout, i.e., areas where fixtures filled with tagged items are located.

The flowchart of the proposed method is depicted in Fig.2. First, the RFID environment is sensed in the four directions of the antennas of the robot. Simultaneously, the SLAM gmapping algorithm [38] is used to build the map while localizing the robot on it. From the last map update, the set of explorable frontiers (F_k) at step k are updated. Next, a frontier f_k is selected from the set of current frontiers, F_k. The heuristic function for the selection of the next explorable frontier, *select_frontier*(F_k), takes as its argument the set of all existing

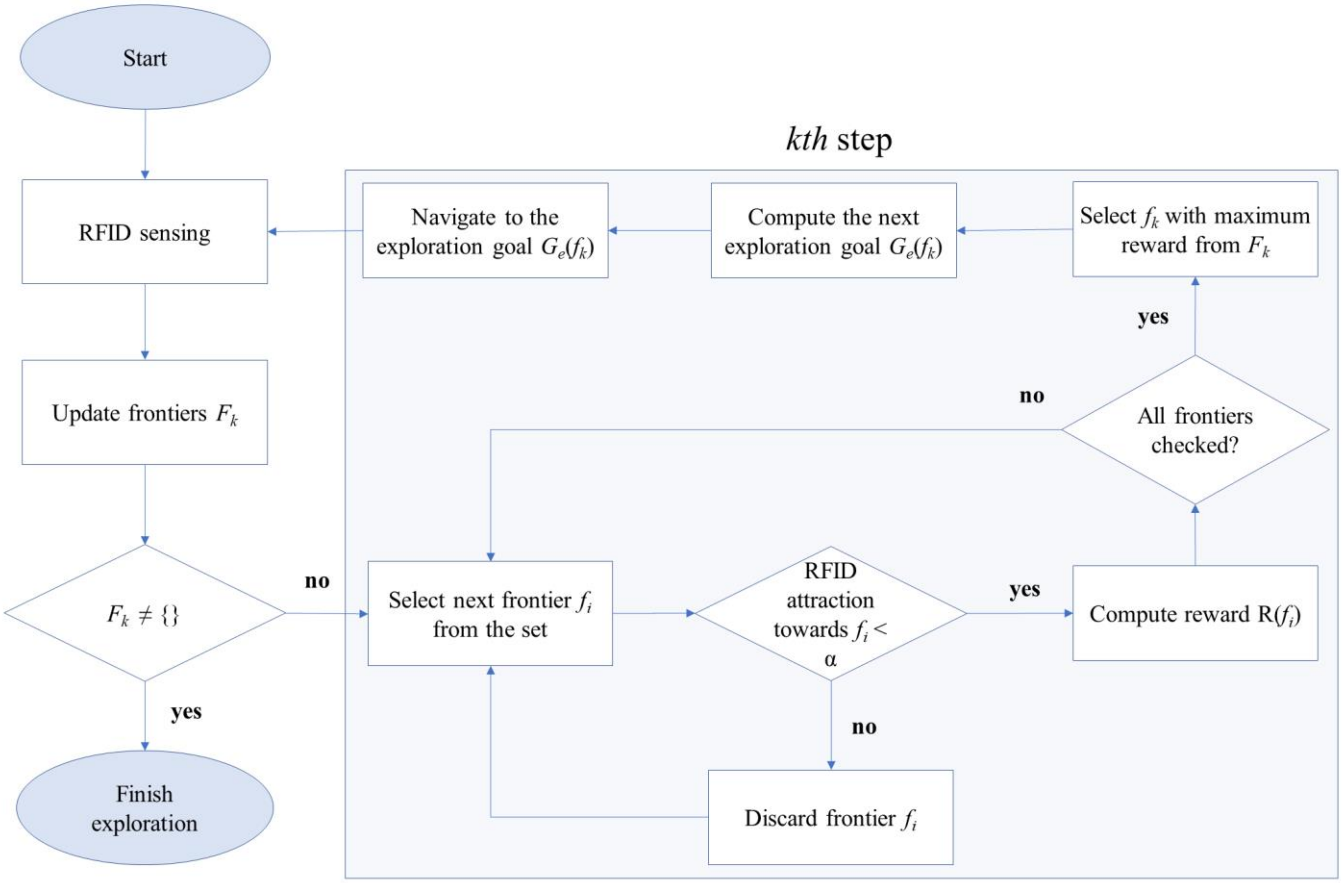

Fig.2. Flowchart of the proposed RFID-based frontier exploration algorithm.

frontiers, $F_k = \{f_1, f_2, \ldots, f_N\}$, and it returns the next frontier, f_k, as a result (see equation 2). This function is intended to obtain the frontier, f_k, with the maximum reward $R(f_k)$ amongst all explorable frontiers. The reward for a specific frontier, $R(f_i)$, is calculated as the quotient between the number of tag readings, obtained in the vicinities of each frontier, and the shortest path distance from the robot to such frontier. The function for the frontier selection is mathematically expressed as:

$$f_k = select\_frontier(F_k) = \underset{f_i}{\operatorname{argmax}}\, R(f_i) = \underset{f_i}{\operatorname{argmax}} \frac{|Tags(f_i)|}{|r_{f_i} - r'|} \quad (2)$$

where the function argmax returns the argument f_i that maximizes $R(f_i)$, $|Tags(f_i)|$ returns the number of different tags read by the robot in the direction of the frontier f_i, from the closest robot pose to such frontier from which f_i has been discovered or updated, $|r_{fi}\text{-}r'|$ accounts for the shortest path distance from the current robot pose r' to the position of the frontier r_{fi}. At each exploration step k, the algorithm checks if a frontier has been discovered or updated, and the 3-tuple (f_i, r', $|Tags(f_i)|$) is stored or updated. And f_i is composed of N frontier cells, $C = \{c_1, c_2, \ldots, c_N\}$, for $N \geq 1$. The frontier cells are obtained using frontier-tracing frontier detection (FTFD) [13]. The exploration goal $G_e(f_k)$, at the step k, is computed as the average value of the positions, c_n, of all cells forming f_k (see equation 3).

$$G_e(f_k) = \frac{1}{N}\sum_{n=1}^{N} c_n \quad (3)$$

Finally, the robot navigates to the exploration goal, after which the kth step concludes. If, at any step, there are no more unexplored frontiers, or the RFID attraction from all frontiers is lower than a specific threshold α, the exploration mission terminates.

In the experiment depicted in Fig.3, a map is built using RFID exploration. The figure illustrates a sequence of steps conducted during an exploration mission (Fig.3(a)-Fig.3(e)). Then, Fig.3(f) illustrates an image representation of the map built during the autonomous exploration. Fig.3(f) shows that the map is automatically constrained to the area of interest of the inventory layout. In contrast, in the map generated by a human operator of Fig.1(c), the map bounds are decided by

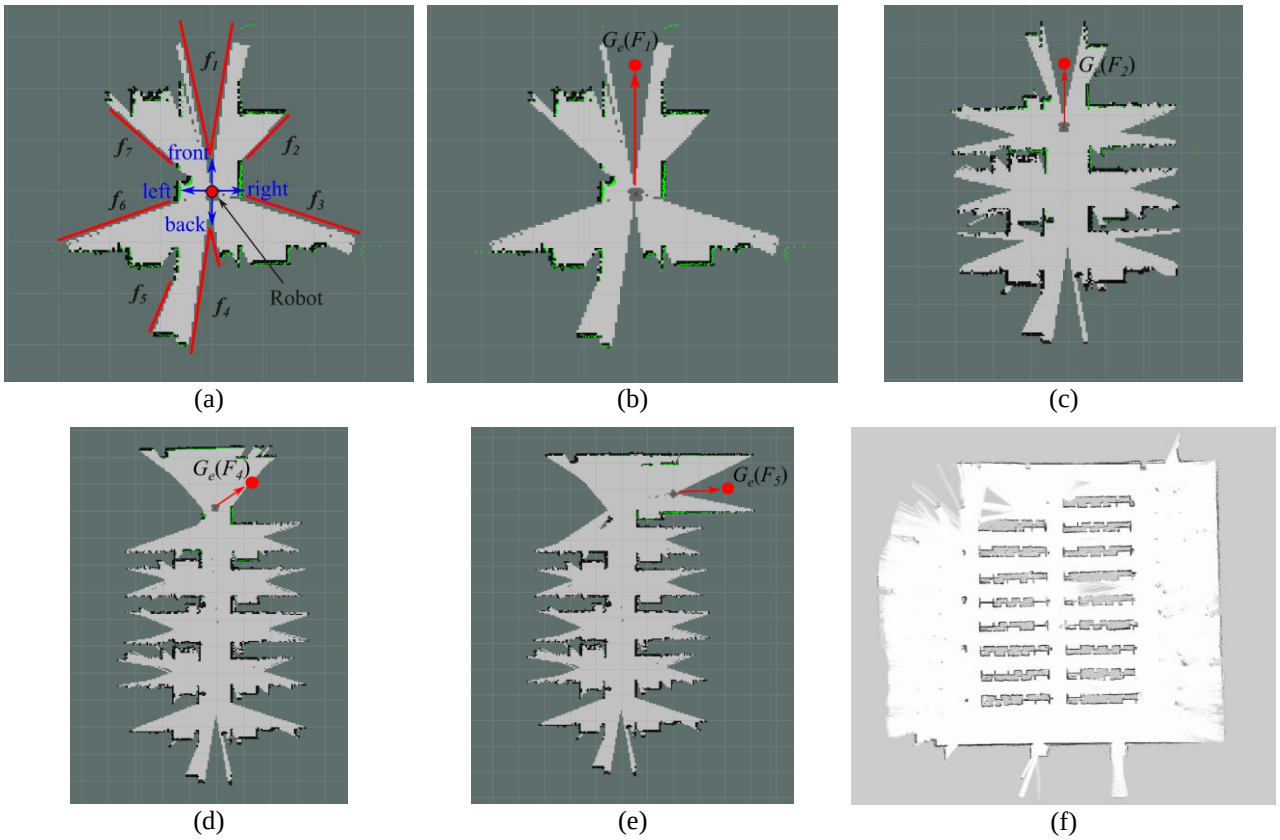

Fig.3. Illustration of an example of the RFID-based autonomous exploration. (a) depicts the schematic of the discovered frontiers at the starting position. At this point, the RFID tag readings are assigned to the different frontiers, F_k, depending on the relative orientation between the robot and the frontier f_i, and the shortest path distance to all frontiers is calculated. (b)-(e) show a series of snapshots at different steps of an exploration mission. (b) corresponds to the first exploration goal, $G_e(F_1)$, which is computed by summing the positions of all cells in the frontier f_1 divided by the number of cells in f_1, and (c), (d) and (e) correspond to steps 2, 4 and 5. (f) Illustrates the image of the map at the end of the exploration mission.

the operator. Consequently, manually generated maps usually contain areas that lack interest from the point of view of the inventory mission. This fact can be observed looking at the distant right and left walls, and the higher left corner of Fig.1(c), which have not been mapped in the autonomous case illustrated in Fig.3(f). It is clear,
then, that this new strategy enables autonomous map building for inventory applications, and it also makes possible to perform an inventory mission while doing the autonomous exploration task. In addition, RFID exploration constrains the map boundaries to the surroundings of the inventory area, and it is expected that it can enable autonomous planning of itineraries for inventory missions.

IV. Waypoint Navigation versus RFID-based Navigation

This section describes four different approaches addressing the inventory problem, namely RFID stigmergy [28], waypoint navigation [29], [39], RFID stigmergy with adaptive Monte Carlo Localization (AMCL) [5], and RFID-based exploration. The last two methods are proposed, for the first time to date, in this contribution.

A. RFID-based navigation

The RFID navigation consists of an ordered series of navigation goals that are obtained in real time, and the set of selected goals depends on the arrangement of the RFID tags around the environment. When a navigation goal is reached, the robot stops and starts sensing the environment for RFID tags in the surroundings during a time interval τ. After τ seconds, the RFID attraction towards each of the four directions, corresponding to the four antennas in the robot, is computed from equation (*4*). This means that the robot can autonomously set goals in one of the following directions: front, left, right and back. And the attraction function returns the rewards for each of the four RFID sensing directions, according to the number of tags read by each antenna. Finally, the navigation goal ($G_{n,k}$) for the step k is obtained at the direction of higher "attraction" (tag readings), from equations 4 and 5.

The attraction, $A(d)$, towards each direction d = {front, right, back, and left} is defined as the number of new tags added to the inventory (n_d) by antenna d, plus all tags read by antenna d (N_d) during the last round, divided by the total number of times that such N_d tags have been read during the whole inventory mission.

$$A(d) = n_d + \frac{N_d}{total(N_d)} \tag{4}$$

$$G_{n,k} = \max_d A(d) \tag{5}$$

Fig.4 displays the instant at which the robot reaches the goal selected at the step k-1 and computes the attraction towards the four directions. TABLE I presents the attraction values sensed from the four antennas for the case illustrated in Fig.4.

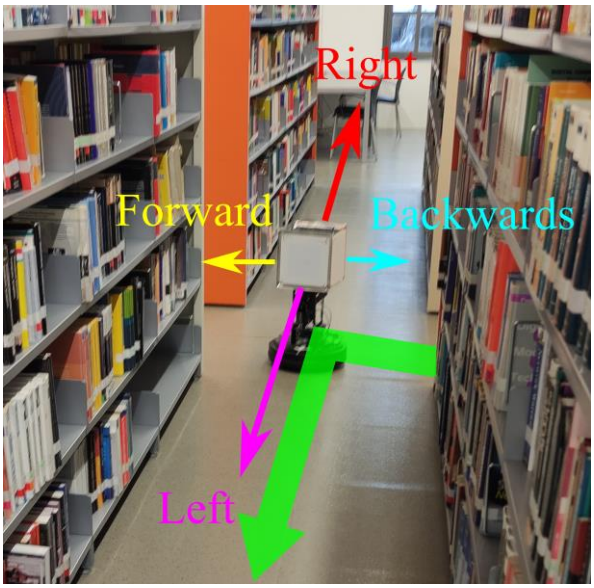

Fig.4. Image of the robot during an inventory mission using RFID-based navigation. The green arrow represents the path of the robot, including the previous route and the next goal. The lengths of the colored arrows (yellow, pink, cyan and red) represent the attraction felt in that direction, according to TABLE I.

TABLE I
EXAMPLE OF THE COMPUTATION OF THE NAVIGATION GOAL

Step	*A*(front)	*A*(left)	*A*(back)	*A*(right)	G_n
***k*-1**	30.0	5.3	3.2	7.3	front
k	10.0	46.1	8.3	34.1	left

The robot localization is performed using the robot odometry with respect to a fixed initial frame. The sensor used in these experiments is a 2D/3D dual solid state time-of-flight (ToF) lidar [32].

An example of an inventory mission using RFID navigation is illustrated in Fig.5. The robot position in the x-y plane is depicted in Fig.5(a). The starting positions for Robot 1 and Robot 2 are (−8, 6) and (8, −6) respectively. As we can observe, the odometry data is not reliable and, therefore, there is a high localization error that makes it difficult to distinguish the library layout from the robot routes. In other words, it's not possible to know exactly which areas have been visited by each of the robots. Although this doesn't affect the inventory performance, having a precise localization can bring important information on the outcome of the stigmergic algorithm. And it would be strictly necessary for stock localization applications. However, inventory localization is out of the scope of this contribution.

In Fig.5(b) the number of unique tags read by each of the robots is depicted along the mission time. As we can see, both robots have similar performance. In this example, the accuracy reaches slightly over 92% by the end of the inventory mission. Finally, we observe that the inventory task is automatically

well balanced between the two robots, each contributing approximately half of the tags.

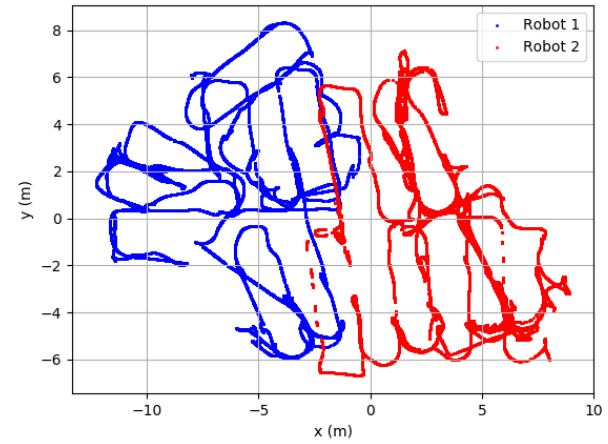

(a)

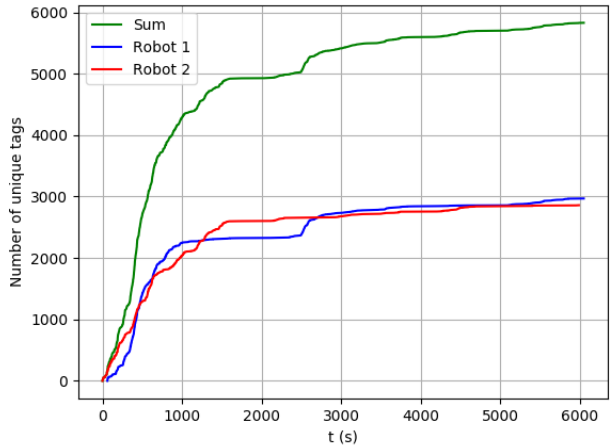

(b)

Fig.5. RFID navigation: (a) odometry-based position estimation collected during an inventory mission using the RFID-based stigmergic navigation and (b) number of unique tags read during the mission by the two robots.

B. Waypoint navigation

This navigation strategy is based on following waypoints in a known map. The map of Fig.1(c) is built using SLAM with a 2D lidar [33]. The robot localizes itself in the map using AMCL. The sensors used during the inventory missions are [33] and [32] for localization and obstacle avoidance respectively.

Two independent robot routes have been designed by a human operator (Fig.6), for each of the robots, to share the inventory area proportionally. The routes avoid direct encounters of the robots, which would impair the navigation, just as any other dynamic obstacle. The routes end at the starting waypoint, so that robots navigate in continuous loops.

Here, Robot 1 starts from waypoint 30 and Robot 2 starts at waypoint 1. Fig.6(b-c) shows the results of an inventory mission using the waypoint navigation strategy. Fig.6(b) plots the robot positions during the inventory mission. We can notice a huge improvement in the robot localization due to the use of AMCL. While the routes are not designed to cross the library central axis, i.e., the line formed by waypoints 2, 5, 8, 11, 14, 17, 20, 23, 26 and 29, eventually the robots cannot plan a straight trajectory to the next waypoint due to the presence of dynamic obstacles. Examples of this issue can be seen for $2 < x < 4$ and $y = 0$, where robot 1 crosses the central axis of the library to reach the next waypoint through another aisle.

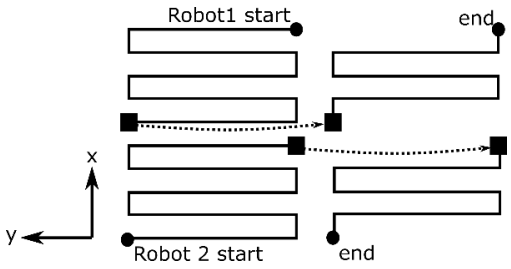

(a)

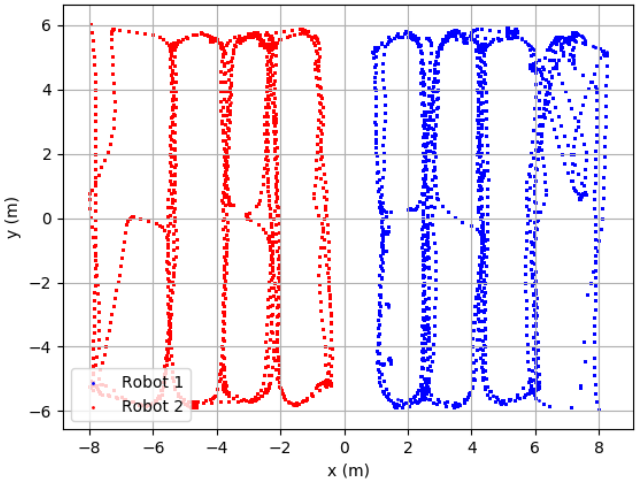

(b)

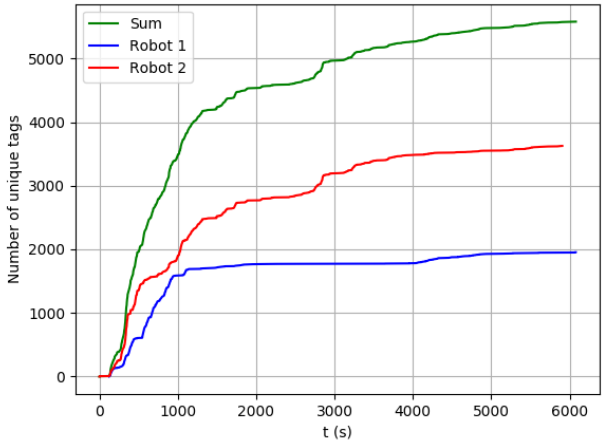

(c)

Fig.6. Waypoint navigation: (a) Illustration of the robot routes for a single loop. The routes are divided in two halves for each robot. Circles mark the starting and ending points. Squares mark the same exact waypoint at the two halves of the route. (b) Robots' positions

following the route of waypoints. (c) Number of unique tags read during the mission by the two robots.

Fig.6(c) depicts the inventory performance of the waypoint navigation and highlights the performance difference between the two robots. The robots' routes are designed to share the inventory area. However, Robot1 reads 1997 tags while Robot2 reads 2792 tags. Robot1 reads fewer tags because its navigation area contains one less shelf than Robot2's area. This difference accounts for approximately 1/10 of Robot2's readings, around 273 tags. However, the main disparity arises from the difference in tag density between the areas traveled by Robot2 and Robot1. This difference is illustrated in Fig.7, which shows the estimated positions of all the tags in the environment, computed using a simple localization technique proposed in [2]. Fig.7 reveals that, for positive x values, the tag density is higher than for negative x values.

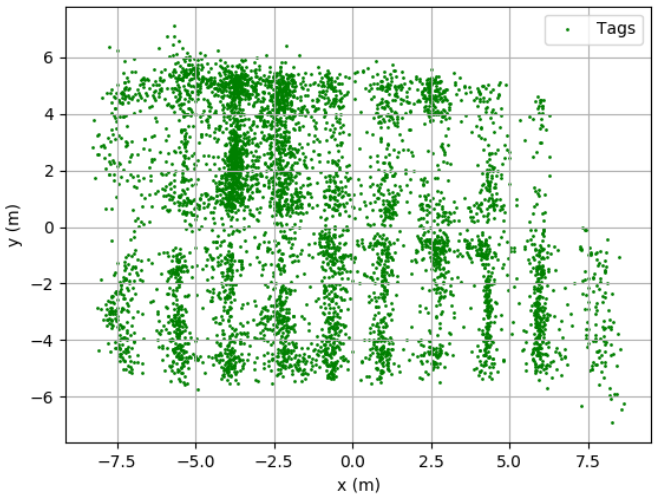

Fig.7. Estimated localization of the tags in the environment using a simple localization technique presented in [2].

C. RFID-based navigation with AMCL

In this case, the robot uses AMCL to provide a better approximation of its own position over time compared to the odometry-based localization used in the simple RFID navigation. The map and the sensors used during these experiments are the same as for the waypoint navigation. This mode provides good localization accuracy that will be useful for analyzing the RFID navigation. An example of the positions of the robots during an inventory mission is illustrated in Fig.8. In this case, Robot 1 (blue dots) starts from (8, −6) and Robot 2 (red dots) starts at (−8, 6).

In this experiment, the length of a complete path covering all the target area is 166 meters. Thus, Fig.8 shows that the robots cover 80.15% of the length of the complete path in the specified mission time (100 min), corresponding to blue and red dots. The coverage is split in 45.2% for Robot 1 and 39.75% for Robot 2, with an inter-robot overlapping of the 4.8%. However, increasing the duration of the experiments lead to higher coverage as proven by mission time extension to 9000 seconds, represented by the orange and green traces (Fig.8). In consequence, the coverage increased to 90.35%. Robot 1 went up to 53.6% and Robot 2 up to 47.6%, while the overlapping also increased to 10.8%.

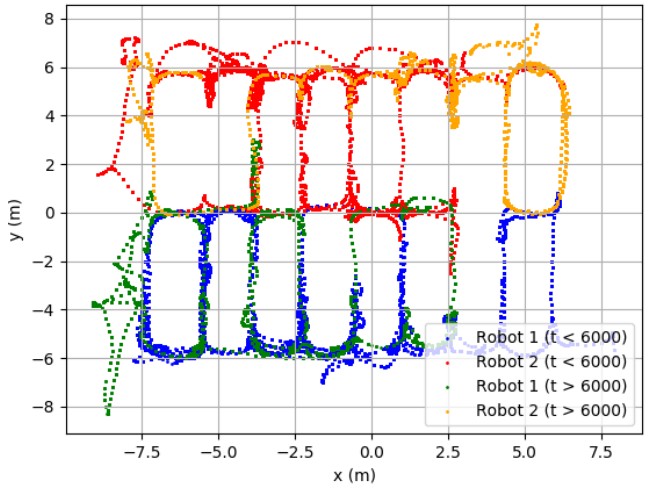

Fig.8. RFID navigation with AMCL: x and y coordinates of the robots poses (Robot 1 in blue and green, and Robot 2 in red and orange).

Fig.8 shows that some of the areas are visited more than once. This is illustrated by a higher density of the tracks, while some previously unvisited aisles have been covered during the time extension. It's worth noticing that some areas are less visited than others. The main reason is that, as illustrated in Fig.7, some areas have a lower density of tags, so the robot doesn't feel attraction towards those areas. Moreover, other nearby areas have a much higher tag density, thus deviating the robot attraction towards the more populated zones.

As already mentioned, in the waypoint navigation, the area corresponding to the central vertical aisle is only partially covered by the robots, unless they find an obstacle that prevents them to traverse the aisle. These differences in the area coverage, between the waypoint-based navigation and the RFID navigation, might not be negligible, since a strong multipath effect is present in RFID inventory environments which could make some tags readable only from specific locations of the map.

Fig.8 brings out another direct consequence of using RFID navigation. That is, an area visited by one robot is rarely visited by the other robot. Thus, each robot covers approximately half of the area of interest. Assuming that the number of robots is properly dimensioned to the inventory area, a robot team made up of the proposed prototypes could scale to very large areas, such as amazon facilities.

D. Comparative analysis

In this section, RFID-based navigation and waypoint-based navigation are compared in terms of inventory performance. Fig.9 shows the results of ten inventory missions, five for each

strategy, shown as red stars. The average of the realizations for each strategy is marked as a blue triangle. The ground truth consists of 6000 tags.

The results show that compared to the waypoint navigation, the RFID-based navigation has slightly higher mean and considerably higher standard deviation in terms of the inventory accuracy. However, in terms of mission time, the waypoint navigation presented much higher deviation and lower average since robots can finish the inventory mission once they complete the mission route. In this scenario, longer times are produced by dynamic obstacles, generally persons walking inside the library.

It is worth mentioning the most common issues encountered during the tests that affected the results. All tests have been performed in a real library, during the hours that it is opened to the public, and therefore, students, cleaning services, security and library staff were walking freely through the library aisles during the missions, which made the navigation task more difficult. In addition, the robots could be momentarily close to each other during the inventory mission. This issue has been demonstrated to be a source of interference for lidar sensors [40], and it actually occurred several times during the experiments.

The consequence of the previous problems is that the navigation stack needs to cope with the dynamic and/or interference-generated obstacles by triggering recovery behaviors or choosing a new goal. This issue can make the routes differ slightly from the expected ones, as we saw in the waypoint navigation subsection, and it can also have an impact on the inventory accuracy.

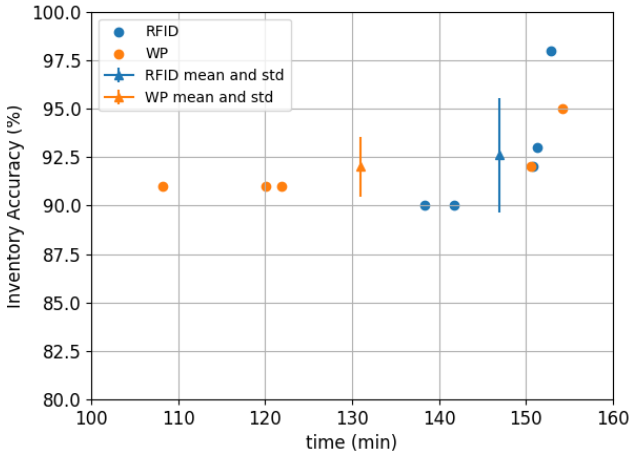

Fig.9. Comparison between the inventory performance following the waypoint navigation (orange dots) and the RFID-based attraction navigation (blue dots).

In the waypoint navigation, the robots do not have to stop and listen to the RFID environment, and they are in constant motion which leads to higher power consumption, but they still must deal with navigation issues such as dynamic obstacles or navigating across narrow aisles. In contrast, when using the RFID navigation strategy, before deciding a navigation goal, robots need a short time (t_{Rx}) to gather the RFID information to compute the attraction function (1). This process has a detrimental impact on the mission performance that depends on the specific time quantity t_{Rx}.

V. Conclusion

This contribution presents 1) a comparison of RFID-based and waypoint-based navigation strategies for inventory robots, and 2) it demonstrates, for the first time to date, the efficacy of RFID stigmergic algorithms to autonomously map inventory areas. It has been proved that the map generated by this approach is not only as accurate as the manually generated map, but that it better adapts to the area of interest corresponding to the zone occupied by the shelves containing the tags.

Two different navigation strategies, namely waypoint navigation and RFID-based navigation have been tested and compared for teams of two robots. RFID-based navigation has proven to achieve similar inventory accuracies than the waypoint navigation strategy in a slightly longer inventory time. But the reader must realize that the RFID-based strategy is fully autonomous. This also implies that, RFID-based navigation does not require re-mapping after layout modifications, which can happen during the battery charging or in the middle of a mission. Particularly, this last case would be especially critical since the robot navigation could fail making the robot navigation crash. In addition, RFID-based navigation is also a better solution for environments with dynamic tag density, where items are rapidly input and output, requiring recursive inspection of specific areas. Therefore, RFID-based navigation is more suitable for perpetual inventory applications, and it enables the scalability of the system that a “plug and play” solution requires.

References

[1] M. Morenza-Cinos, V. Casamayor-Pujol, and R. Pous, “Stock visibility for retail using an RFID robot,” *IJPDLM*, vol. 49, no. 10, pp. 1020–1042, Dec. 2019, doi: 10.1108/IJPDLM-03-2018-0151.

[2] V. Casamayor-Pujol, B. Gaston, S. Lopez-Soriano, A. A. Alajami, and R. Pous, “A Simple Solution to Locate Groups of Items in Large Retail Stores Using an RFID Robot,” *IEEE Trans. Ind. Inf.*, vol. 18, no. 2, pp. 767–775, Feb. 2022, doi: 10.1109/TII.2021.3080670.

[3] A. Kamalova, K. D. Kim, and S. G. Lee, “Waypoint Mobile Robot Exploration Based on Biologically Inspired Algorithms,” *IEEE Access*, vol. 8, pp. 190342–190355, 2020, doi: 10.1109/ACCESS.2020.3030963.

[4] J. Zhang, Y. Lyu, T. Roppel, J. Patton, and C. P. Senthilkumar, “Mobile robot for retail inventory using RFID,” in *2016 IEEE International Conference on Industrial Technology (ICIT)*, Taipei, Taiwan: IEEE, Mar. 2016, pp. 101–106. doi: 10.1109/ICIT.2016.7474733.

[5] S. Thrun, “Probalistic Robotics20062D.M. Hutton Computer Science International, UK(Section Editor). *Probalistic Robotics* . MIT Press, 2006. 668 pp., ISBN: 0-262-20162,”

Kybernetes, vol. 35, no. 7/8, pp. 1299–1300, Aug. 2006, doi: 10.1108/03684920610675292.

[6] J. Clemens, T. Reineking, and T. Kluth, "An evidential approach to SLAM, path planning, and active exploration," *International Journal of Approximate Reasoning*, vol. 73, pp. 1–26, 2016, doi: https://doi.org/10.1016/j.ijar.2016.02.003.

[7] P. K. Panigrahi and S. K. Bisoy, "Localization strategies for autonomous mobile robots: A review," *Journal of King Saud University - Computer and Information Sciences*, p. S1319157821000550, Mar. 2021, doi: 10.1016/j.jksuci.2021.02.015.

[8] D. Perea Ström, I. Bogoslavskyi, and C. Stachniss, "Robust exploration and homing for autonomous robots," *Robotics and Autonomous Systems*, vol. 90, pp. 125–135, Apr. 2017, doi: 10.1016/j.robot.2016.08.015.

[9] Y. Chen, S. Huang, and R. Fitch, "Active SLAM for Mobile Robots With Area Coverage and Obstacle Avoidance," *IEEE/ASME Trans. Mechatron.*, vol. 25, no. 3, pp. 1182–1192, Jun. 2020, doi: 10.1109/TMECH.2019.2963439.

[10] C. Papachristos *et al.*, "Autonomous Exploration and Inspection Path Planning for Aerial Robots Using the Robot Operating System," in *Robot Operating System (ROS)*, A. Koubaa, Ed., in Studies in Computational Intelligence, vol. 778. Cham: Springer International Publishing, 2019, pp. 67–111. doi: 10.1007/978-3-319-91590-6_3.

[11] N. Yu and S. Wang, "Enhanced Autonomous Exploration and Mapping of an Unknown Environment with the Fusion of Dual RGB-D Sensors," *Engineering*, vol. 5, no. 1, pp. 164–172, Feb. 2019, doi: 10.1016/j.eng.2018.11.014.

[12] B. Fang, J. Ding, and Z. Wang, "Autonomous robotic exploration based on frontier point optimization and multistep path planning," *IEEE Access*, vol. 7, pp. 46104–46113, 2019, doi: 10.1109/ACCESS.2019.2909307.

[13] P. Quin, D. D. K. Nguyen, T. L. Vu, A. Alempijevic, and G. Paul, "Approaches for Efficiently Detecting Frontier Cells in Robotics Exploration," *Front. Robot. AI*, vol. 8, p. 616470, Feb. 2021, doi: 10.3389/frobt.2021.616470.

[14] H. Tang, W. Sun, H. Yu, A. Lin, and M. Xue, "A multirobot target searching method based on bat algorithm in unknown environments," *Expert Systems with Applications*, vol. 141, p. 112945, Mar. 2020, doi: 10.1016/j.eswa.2019.112945.

[15] H. Li, Q. Zhang, and D. Zhao, "Deep Reinforcement Learning-Based Automatic Exploration for Navigation in Unknown Environment," *IEEE Trans. Neural Netw. Learning Syst.*, vol. 31, no. 6, pp. 2064–2076, Jun. 2020, doi: 10.1109/TNNLS.2019.2927869.

[16] J. J. Lopez-Perez, U. H. Hernandez-Belmonte, J.-P. Ramirez-Paredes, M. A. Contreras-Cruz, and V. Ayala-Ramirez, "Distributed Multirobot Exploration Based on Scene Partitioning and Frontier Selection," *Mathematical Problems in Engineering*, vol. 2018, pp. 1–17, Jun. 2018, doi: 10.1155/2018/2373642.

[17] "EPC™ Radio-Frequency Identity Protocols, Generation-2 UHF RFID Standard, Specification for RFID Air Interface Protocol for Communications at 860 MHz – 960 MHz, Release 2.1, Ratified, Jul 2018." https://www.gs1.org/standards/rfid/uhf-air-interface-protocol (accessed May 16, 2023).

[18] Ö. E. Çakıcı, H. Groenevelt, and A. Seidmann, "Using RFID for the management of pharmaceutical inventory — system optimization and shrinkage control," *Decision Support Systems*, vol. 51, no. 4, pp. 842–852, Nov. 2011, doi: 10.1016/j.dss.2011.02.003.

[19] T.-J. Fan, X.-Y. Chang, C.-H. Gu, J.-J. Yi, and S. Deng, "Benefits of RFID technology for reducing inventory shrinkage," *International Journal of Production Economics*, vol. 147, pp. 659–665, Jan. 2014, doi: 10.1016/j.ijpe.2013.05.007.

[20] T. Fan, F. Tao, S. Deng, and S. Li, "Impact of RFID technology on supply chain decisions with inventory inaccuracies," *International Journal of Production Economics*, vol. 159, pp. 117–125, Jan. 2015, doi: 10.1016/j.ijpe.2014.10.004.

[21] B.-S. Choi, J.-W. Lee, J.-J. Lee, and K.-T. Park, "A Hierarchical Algorithm for Indoor Mobile Robot Localization Using RFID Sensor Fusion," *IEEE Trans. Ind. Electron.*, vol. 58, no. 6, pp. 2226–2235, Jun. 2011, doi: 10.1109/TIE.2011.2109330.

[22] A. Tzitzis *et al.*, "Localization of RFID Tags by a Moving Robot, via Phase Unwrapping and Non-Linear Optimization," *IEEE J. Radio Freq. Identif.*, vol. 3, no. 4, pp. 216–226, Dec. 2019, doi: 10.1109/JRFID.2019.2936969.

[23] A. Raptopoulos Chatzistefanou, A. Tzitzis, S. Megalou, G. Sergiadis, and A. G. Dimitriou, "Trajectory-Tracking of UHF RFID Tags, Exploiting Phase Measurements Collected From Fixed Antennas," *IEEE J. Radio Freq. Identif.*, vol. 5, no. 2, pp. 191–206, Jun. 2021, doi: 10.1109/JRFID.2021.3053101.

[24] R. Polvara, M. Fernandez-Carmona, G. Neumann, and M. Hanheide, "Next-Best-Sense: A Multi-Criteria Robotic Exploration Strategy for RFID Tags Discovery," *IEEE Robot. Autom. Lett.*, vol. 5, no. 3, pp. 4477–4484, Jul. 2020, doi: 10.1109/LRA.2020.3001539.

[25] H. Wu, B. Tao, Z. Gong, Z. Yin, and H. Ding, "A Standalone RFID-Based Mobile Robot Navigation Method Using Single Passive Tag," *IEEE Trans. Automat. Sci. Eng.*, pp. 1–9, 2020, doi: 10.1109/TASE.2020.3008187.

[26] B. Rahmadya, R. Sun, S. Takeda, K. Kagoshima, and M. Umehira, "A Framework to Determine Secure Distances for Either Drones or Robots Based Inventory Management Systems," *IEEE Access*, vol. 8, pp. 170153–170161, 2020, doi: 10.1109/ACCESS.2020.3024963.

[27] A. Kleiner, J. Prediger, and B. Nebel, "RFID Technology-based Exploration and SLAM for Search And Rescue," in *2006 IEEE/RSJ International Conference on Intelligent Robots and Systems*, Beijing, China: IEEE, Oct. 2006, pp. 4054–4059. doi: 10.1109/IROS.2006.281867.

[28] V. Casamayor-Pujol, M. Morenza-Cinos, B. Gastón, and R. Pous, "Autonomous stock counting based on a stigmergic algorithm for multi-robot systems," *Computers in Industry*, vol. 122, p. 103259, 2020, doi: https://doi.org/10.1016/j.compind.2020.103259.

[29] Y. Wang, D. Mulvaney, I. Sillitoe, and E. Swere, "Robot Navigation by Waypoints," *J Intell Robot Syst*, vol. 52, no. 2, pp. 175–207, Jun. 2008, doi: 10.1007/s10846-008-9209-6.

[30] "Turtlebot 2." https://www.turtlebot.com/turtlebot2/ (accessed May 16, 2023).

[31] "raspberry pi 4 model B." https://www.raspberrypi.org/products/raspberry-pi-4-model-b/ (accessed May 16, 2023).

[32] "cyglidar." https://www.cygbot.com/2d-3d-dual-solid-state-tof-lidar (accessed May 16, 2023).

[33] "ydlidar x4." https://www.ydlidar.com/products/view/5.html (accessed May 16, 2023).

[34] "Advanreader 160." https://wiki.keonn.com/rfid-components/advanreader-160 (accessed May 16, 2023).

[35] "Advantenna-SP11." https://wiki.keonn.com/rfid-components/antennas (accessed May 16, 2023).

[36] "UPF library." https://www.upf.edu/es/web/biblioteca-informatica/poblenou (accessed May 16, 2023).

[37] B. Gaston, V. Casamayor-Pujol, S. Lopez-Soriano, and R. Pous, "A metric for assessing, comparing and predicting the performance of autonomous RFID-based inventory robots for

retail," *IEEE Trans. Ind. Electron.*, pp. 1–1, 2022, doi: 10.1109/TIE.2021.3128917.
[38] "gmapping." https://openslam-org.github.io/gmapping.html (accessed May 16, 2023).
[39] N. M. Ben Lakhal, L. Adouane, O. Nasri, and J. Ben Hadj Slama, "Safe and adaptive autonomous navigation under uncertainty based on sequential waypoints and reachability analysis," *Robotics and Autonomous Systems*, vol. 152, p. 104065, Jun. 2022, doi: 10.1016/j.robot.2022.104065.
[40] I.-P. Hwang and C.-H. Lee, "Mutual Interferences of a True-Random LiDAR With Other LiDAR Signals," *IEEE Access*, vol. 8, pp. 124123–124133, 2020, doi: 10.1109/ACCESS.2020.3004891.

S. López-Soriano received the M.Sc. degree in Micro and Nanoelectronics Engineering and the Ph.D. degree in Electronics and Telecommunication Engineering from the Universitat Autònoma de Barcelona (UAB), Bellaterra, Spain, in 2013 and 2018 respectively. From 2018 to 2019 he was a postdoctoral researcher at the LCIS Laboratoire of the Grenoble INP. From 2019 to 2022 he was a researcher at the Universitat Pompeu Fabra. Currently, he is a post-doctoral researcher in the Universitat Oberta de Catalunya. His current research interests include RFID systems, robotics and antenna-based sensors.

Rafael Pous received a B.S. in Telecommunications Engineering and a B.S. in Computer Science from the Technical University of Catalonia, in 1988. In 1989 he received a Ms.C. in Electrical Engineering from the University of Massachusetts at Amherst. In 1992 he received Ph.D. in Electrical Engineering from the University of California at Berkeley. From 1993 to 2009 he was an Associate Professor at the Technical University of Catalonia, and since 2009 he was an Associate Professor at Pompeu Fabra University. Since 2021, he is a Full Professor at Pompeu Fabra University. His past research interests included numerical methods in electromagnetism, applied superconductivity, and fractal antennas. His current research is focused on Ubiquitous Computing and the Internet of Things applied to different industries, using RFID and robotics, among other technologies. In parallel to his academic career, he has cofounded 3 technology start-up companies.